Monitoring the Film Formation Process of Polystyrene/Poly Acrylamide (PS/PAAm) Composite Films Annealed by IR Heating

Ali Gelir,[1] Onder Yargi,[2] Berkay Sarli,[2] Utkan Sahinturk,[3] Baki Aksakal[2]
[1] *Department of Physics, Istanbul Technical University, Maslak, Istanbul, 34469, Turkey*
[2] *Department of Physics, Yildiz Technical University, Esenler, Istanbul, 34210, Turkey*
[3] *Machine Programme, Department of Mechanical and Metal Technology, Vocational School of Technical Sciences, Istanbul University, Istanbul, TR-34320, Turkey*

In this study, UV-visible(UVV) technique was used to probe the evolution of optical transmission during the film formation from composites of polystyrene (PS) latex particles and poly acrylamide (PAAm) films annealed by the infrared radiative heating (IRH) and convectional heating. Activation energies corresponding to the void closure and the interdiffusion stages were calculated. It was shown that the activation energy for the void closure processes of viscous flow from the composite films decreased considerably in IRH annealing technique. It was observed that IRH heating speeds up the film formation process and the decrease the required energy. POLYM. ENG. SCI., 00:000–000, 2017. © 2017 Society of Plastics Engineers

INTRODUCTION

Nowadays, radiation from infrared sources has gained attention especially for heating. IR radiation has been applied to dry foods [1] and waterborne polymers [2, 3]. IR radiant heating is used extensively in industry, particularly for drying of materials or fusing of coatings (powder coating, drying of paints or printed layers). Infrared heating can be defined as applying radiant energy to an object by direct transmission from an emitter (source). Some of the energy emitted will be reflected off the surface, some is absorbed by the substrate and some is transmitted through the substrate. The absorption characteristics depend on the type of the material, the color, and the surface finish. The actual behavior of IR energy depends on the wavelength, the distance between the substrate and the emitter, the mass of the object, the surface area and the color sensitivity. Generally shorter wavelength infrared radiation penetrates further into the substrate but is more sensitive to changes in the color of the substrate. Generally speaking, polymers absorb more effectively in the medium IR range (this is the frequency more commonly employed in powder coating applications for example) [4]. The drying time of aqueous solutions of poly (vinyl alcohol) was reduced from 120 min, which is for convective drying, to only 15 min for combined convective and IR radiative drying [2].

IR heating has some advantages comparing with the heating with convection [5]. First, the slow rate of heat transfer through air in convective heating leads to long heat-up times in convection ovens. Using infrared emitters, it is possible to heat surfaces rapidly due to high transfer of energy and minimize the conduction losses. Second, the combustion products, recirculation of dust, *etc*. make convective heating unsuitable for "clean" applications. Since the IR heating does not produce any combustion and does not need any recirclation of air, it is clearer than the convectional heating. Third, the time to reach the operating temperature for the convection ovens is lasts from 30 minutes to 2 h depending on the size of the convection oven which means that the oven must be turned on to reach the required temperature much before the experiment. But for infrared emitter, this time is very short because it can be switched on and off within very short time intervals and by adjusting the electrical voltage applied on the emitter, it can reach the operating temperature in a very short time. Fourth, in convective heating in an oven, heat diffuses from the film surface and the time for homogeneous distribution of temperature through the film directly depends on this heat diffusion. In addition, evaporation rate of water in waterborne coatings for the film formation is faster when IR radiation heating is used instead of heating by convection. Fifth, the emitted radiation from IR source is only absorbed by the substrate (or treated portions of the substrate) and not by the surrounding air or objects [6].

In another study, microwave heating was applied to the mixture of the polymer (PS) and carbon nanotubes and a better dispersion of the carbon nanotubes in the polymer matrix was obtained. This homogeneous dispersion increased the electrical conductivity of the nanotubes [7]. On the other hand, both IRH and standard heating in the oven were used to cure the colloids before drying. No significant difference on the curing kinetics observed between IRH and the oven if the mean temperature conditions are the same [8]. However, in our study, IR radiant effect was investigated after drying of colloids on glass substrates and considerable difference was observed between IRH and oven.

Latex films are generally formed by coalescence of submicrometer polymer particles in the form of a colloidal dispersion, usually in water. Aqueous dispersions of colloid particles with T_g below the drying temperature known as low-T latex (soft latex in which the particles are of submicrometre size). To understand the mechanism of homogeneous film formation from latex particles is quite important for enhancing the quality of coatings. Traditionally, the film formation process of polymer latex is considered in terms of three sequential steps: (i) Colloid concentration increases as water evaporates, a uniform shrinkage of the interparticle distance occurs, and the voids are gradually filled by particle sliding until a dense packing of spheres is

Correspondence to: O. Yargi; e-mail: oyargi@yildiz.edu.tr
DOI 10.1002/pen.24581
Published online in Wiley Online Library (wileyonlinelibrary.com).
© 2017 Society of Plastics Engineers

obtained. (ii) Deformation of the particles and close contact between the particles if their T_g is less than or close to the drying temperature (soft or low T_g latex). Latex with a T_g above the drying temperature (hard or high T_g latex) stays undeformed at this stage. Annealing of a hard latex system above the minimum film formation temperature, deformation of particles first leads to void closure [7, 8] and then after the voids disappear, diffusion across particle–particle boundaries starts, i.e., the mechanical properties of hard latex films evolve during annealing. Particles are deformed to polyhedrons where the deformation is driven by the combination of surface and osmotic forces until all solvent has evaporated and all voids have disappeared. This process is called coalescence. (iii) After void closure is completed, film formation is known interdiffusion by annealing of hard latex, coalescence of the deformed particles to form a homogeneous film [8] where macromolecules belonging to different particles mix by interdiffusion [9, 10]. This understanding of latex film formation can now be exploited to underpin the processing of new types of coatings and adhives. The blending of latex particles and inorganic nanoparticles provides a facile means of ensuring dispersion at the nanometer scale in composite coatings.

Film formation from latexes was studied using various experimental techniques such as electron [11] and atomic force microscopies [12], neutronscattering [13], nonradiative energy transfer conjunction with time resolved [14], and steady state fluorescence [15]. Light has been used to monitor the film formation for a long time. Ellipsometry [16], photon transmission [17–19] and reflection [20] techniques have been elaborated for latex film formation processes. Scanning [21] and transmission [22] electron microscopies and some reviews [23, 24] have been commonly used techniques to characterize the latex systems. In some of previous studies, IRH heating was used for latexes of aqueous solutions during drying or powder form of polymers [2, 4]. There is no so much information about after drying process of latexes using IRH technique.

In this work, we investigated the film formation from pure Polystyrene (PS) and Polystrene/Polyacrylamide (PS/PAAm) composites depending on two different heating processes, IRH and convective heating after drying of aqueous solutions. The film formation processes were monitored by using photon transmission (PT) technique. PS was chosen as main constituent because of being easily processes, solubility in a broad range of solvents and its clarity which allows dispersion of PAAm to be optically observable at the micron scale. In some works in literature the technological applications of PS were emphasized. For example, electromagnetic interference (EMI) shielding effectiveness provided by the polymer (PS) foam composite with just 7 wt% CNT loading was around 20 dB. This clearly implies that such a CNT-PS foam composite can be used commercially as a shielding material against electromagnetic radiation [25]. Also, review articles about the composites of PS with different organic molecules and structures [26], the composites of PS and lignin as a reinforcement agent [27], the behavior of the metal nanoparticles embedded in PS matrix [28], and the technological potential of PS/Clay composites [29] can be reached in literature.

After each annealing step, the transmitted light intensity, I_{tr}, was monitored by using UV-Visible (UVV) technique to observe the film formation in two seperate heating conditions. The increase in I_{tr} was explained by the activation energy of viscous flow (void closure) up to healing temperature, T_h, and above T_h it was explained by the backbone activation energy of interdiffusing polymer chains processes for both IRH and convective heating.

EXPERIMENTAL

Materials

Polysterene, (PS). Fluorescent PS latexes were prepared via a surfactant free emulsion polymerization process of styrene monomer (99% pure from Alfa Asea) using (Potassium persulphate) KPS as initiator. The fluorescent latexes were prepared by adding fluorescent monomer dimethacrylate (PolyFluorTM 511 from Polysciences, Inc.) in polymer solution. The water-soluble radical initiator KPS was dissolved in water and added when the polymerization temperature reached 90°C. In all polymerizations, deionized water was used.

Poly Acrylamide, (PAAm). The monomer, acrylamide (AAm); the initiator, ammonium persulphate (APS); and the multifunctional crosslinkers, methylenebisacrylamide (Bis) were supplied by Merck (Darmstadt, Germany). All chemicals were used as received. PAAm polymer was prepared by dissolving 0.5 M AAm in bidistilled water in the presence of 7.0 mM APS. The sample solution was sealed by a Teflon stopper after deoxygenation by nitrogen during 15 minutes. Then, the sample was put in a heat bath at 60°C.

Film Preparation. Two sets were prepared from the dispersion of PS/PAAm composites by placing the same number of drops on a glass plates with the size of 1.4×2.5 cm^2 and allowing the water to evaporate. One set was prepared for the convective heating and the other set was prepared for IRH. Then the samples were separately annealed starting from 60°C below T_g of PAAm to 270°C for 10 min in both oven and under IR lamb. The temperature was maintained within ± 2°C during annealing for oven and ± 1°C for IRH.

Measurements

UV-Visible (UVV). Photon transmission measurements were performed by using UV-Visible spectrometer, B&W Tek. The transmittances of the films were detected at 800 nm. A glass plate was used as a standard for all transmittance experiments and measurements were carried out at room temperature after each annealing processes Scanning Electron Microscopy (SEM) images of pure PS and PS/PAAm composites were obtained by Philips XL30 SFEG probe microscopy.

Scanning Electron Microscopy (SEM). SEM analysis was used to investigate the morphology and the microstructure of PS and PS/PAAm films. Non-conductive specimens were mounted on aluminium stubs using carbon tape and they are coated with gold by using a Polaron SC7610 Sputter in vacuum before the examination in the SEM The surface morphology of the composite films were examinated by Philips XL30 SFEG scanning electron microscope (SEM) at 5 kV.

 DOI 10.1002/pen

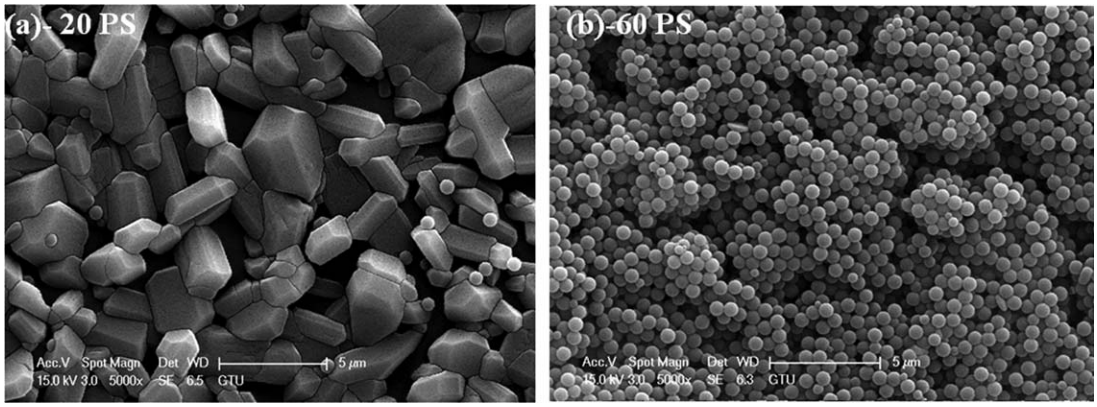


FIG. 1. SEM images of (a) 20 PS (wt%) and (b) 60 PS (wt%) content in PS/PAAm composite films at room temperature.

RESULTS AND DISCUSSION

SEM images given in Fig. 1a and b show the structures of the film with low PS (20 wt%) and high PS (60 wt%) contents before the annealing at room temperature, respectively. It is seen that the structure of the polymer particles are completely different for each polymers. The structure is generally in rectangular prism form for PAAm and it is in spherical form for PS particles. The average length, 2.35 ± 0.62 μm, of the PAAm particles in rectangular prism form is bigger than the average diameter, 0.63 ± 0.03 μm, of the spherical PS particles.

Transmitted photon intensities, I_{tr}, at 800 nm from the latex films with changing PS concentrations and with changing annealing temperatures for the samples annealed in the oven and in IRH are shown in Fig. 2. For low PS contents, (5, 10, partly 20 wt%), I_{tr} is high and nearly constant at the initial annealing temperatures and then decreases upon increasing annealing temperature. The high I_{tr} at the initial annealing temperatures for low PS contents may be explained as follows: The average size of the PAAm particles are big (around a few micrometers as seen in Fig. 1a) when compared with the wavelength of the light passing through the film. This property makes the film nearly nonscattering medium for the light passing through it. When the film is annealed, the average particle size of the PAAm particles start to decrease (Fig. 6) and the structure of the film start to transform to a scattering medium. Thus, the transmitted light intensity descreases upon annealing for the films with low PS content. Another important point here is that the temperature range at which the transmitted light intensity is constant is wider for the films annealed in the oven. This clearly shows that the thermal energy was absorbed by the films more effectively in IRH annealing system for this range. For the other PS concentrations in Fig. 2, I_{tr} is low at the initial annealing tempertures and it starts to increase after a certain onset temperature, called the minimum film formation temperature T_o, and then reaches a maximum with increasing annealing temperature. Finally, it decreases above T_h. The low I_{tr} at the initial stage shows that the structure of the film becomes heterogeneous due to the doped PS particles because PS particles behave like scattering centers for the light. When the temperature is increased, the polymer particles start to flow through the voids rapidly and the film starts to turn to more homogeneous structure. This process is called as the void closure; i.e., polymer starts to flow upon annealing and the voids between the particles can be filled. Spherical particles that have increasing the surface energy flow to intervoids at early stages of the annealing, where the radius

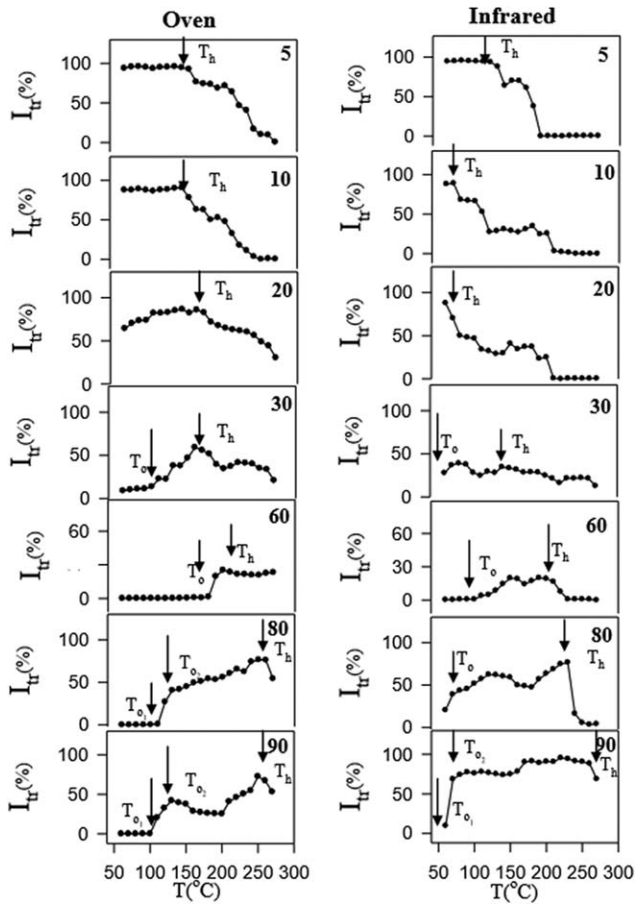


FIG. 2. Transmitted light intensity (*I*tr) versus temperature for PS/PAAm composite films annealed by the conventional heating in the oven and by IRH system. The numbers 5 to 90 in each plot denotes the PS content in the film.

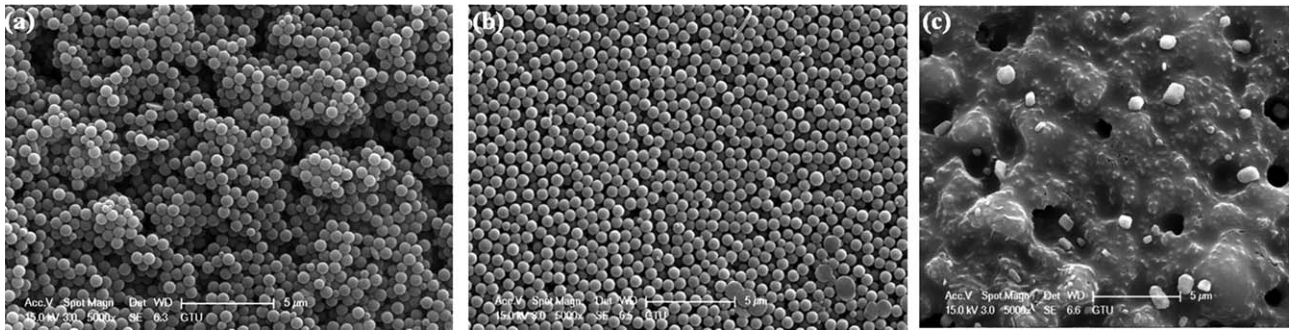


FIG. 3. SEM images of the composite films with 60 PS (wt%) content before annealing (a) and after annealing at 150°C (b and c). The composite films given in (b) and (c) were annealed in the oven and in IRH system, respectively.

of the interparticle voids becomes smaller and the film surface becomes more homogeneous; consequently, transparancey of the films starts to increase. If the annealing is continued, minor chains move across the particle-particle interfaces, and therefore, the latex film becomes more transparent. This process is called healing between T_o and $T_{h.}$ At higher temparatures, the chains gain sufficient kinetic energy to transform its centre of mass across the junction surface (interdiffusion) above T_h [30].

The void closure process is clearly visible in the SEM images given in Fig. 3. These images were given as an example and they belong to the films with 60 PS (wt%) content before the annealing, and after the annealing at 150°C in the oven and in the IRH system. Here, upon annealing the films, PS particles in the PS clusters starts to move towards the voids between the clusters and the voids almost disappeared as seen in Fig. 3b. The difference between the annealing systems can also be seen from the images given in Fig. 3b and c. Although the annealing temperatures are equal for both annealing systems, almost the healing process is started for the film annealed in IRH while the void closure process is nearly completed for the film annealed in the oven. This clearly shows that the efficiency of the heat transport is more efficient in IRH system as mentioned before and the film formation process can be performed at lower temperatures. This point is also observed in the transmitted light measurements and will be discussed below.

In Fig. 4, the onset and the healing temperatures for the films annealed in the oven and in the IRH were shown depending on the PS content of the films. As seen from Fig. 4a that T_o values for the oven are higher than the IRH which is in accordance with the results of our previous work [31]. This clearly indicates that the annealing the films in the IRH system decreases the required temperature to start the film formation process as mentioned above. Another point in this figure is that, T_o values increase up to 60 PS (wt%) content and then decrease for both systems as seen in Fig. 4a. This situation is attributed to a phase separation which is more effective in the low PS content, i.e., the PS particles behave like a scattering centers at low concentration and the onset temperature increases as a result of increasing PS concentration until a specific concentration. Above this specific concentration, PS particles become dominant and the

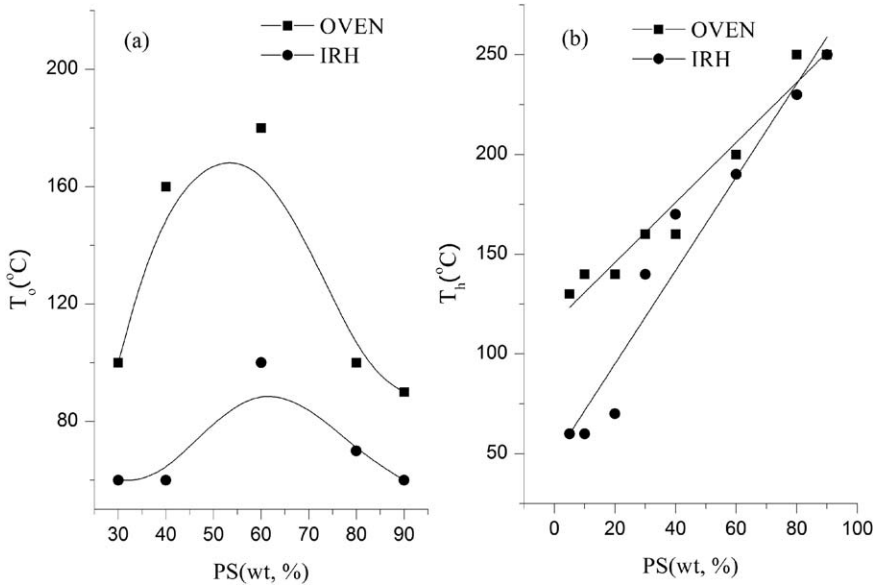


FIG. 4. The minimum film formation temperature, *T*o, (a), and the healing temperature, *T*h, (b) versus PS (wt%) content for the films annealed by the conventional heating in the oven and IRH system.

 DOI 10.1002/pen

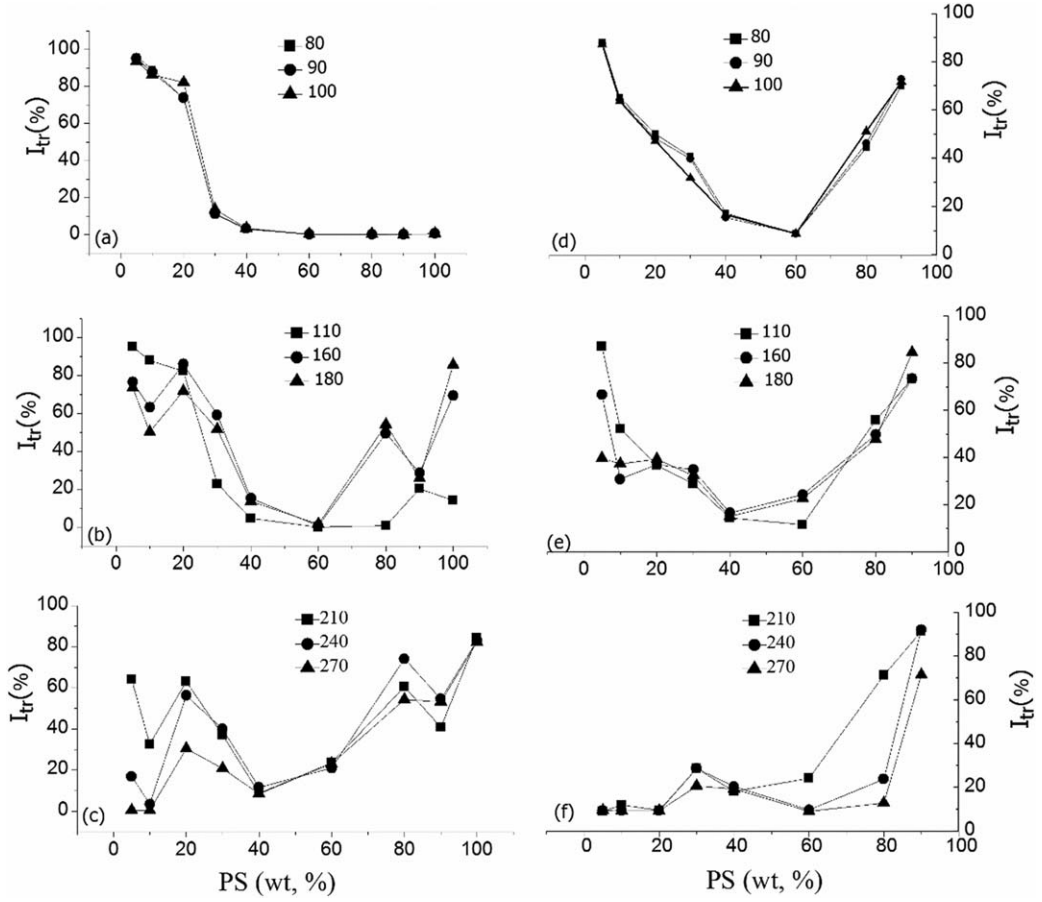


FIG. 5. Transmitted light intensity (*I*tr) versus PS (wt%) content for the films annealed by the conventional heating in the oven (a, b, c) and in IRH system (d, e, f). The numbers in the legend in each figure denote the annealing temperatures for the films.

voids can be closed easier by the huge amount of PS particles which results in a decreasing onset temperature. As seen in Fig. 4b that the healing temperatures for the oven are higher than those for the IRH especially for the low PS contents (below 30 wt%) and the healing temperatures are nearly equal for the higher PS contents. This result may show that the thermal energy emitted by the IR lamp is absorbed more efficiently by the PAAm particles. At low PS concentrations, since the thermal energy is absorbed more efficiently by the PAAm particles, the healing process is achieved at lower temperatures. But at high PS concentrations, PS particles disturb this efficient energy absorbtion and results in an increasing healing temperature.

In Fig. 5, the variation of I_{tr} with the PS content at different annealing temperatures for both annealing systems are represented. At low temperatures, below 110°C, the void closure process probably cannot be completed in the oven and the films are highly heterogeneous for the higher PS contents which results in lower transmitted light intensity as seen in Fig. 5a. This point is proved by the SEM images given in Fig. 3b. It is seen in this figure that the voids in the film annealed in the oven can only be closed at around 150°C. However, the films annealed with IRH, the void closure process is completed as seen in Fig. 3c due to the more effective heat transport and the transmitted light intensity increased with the PS content above 60% PS as seen in Fig. 5d. This clearly shows that the film formation process can be performed at lower temperatures in IRH system as mentioned before. Below 210°C, I_{tr} decreases upto 60% PS content and then increases for both annealing systems. The reason for the decrease in I_{tr} for the low PS concentration is the increasing scattering probability of the PAAm particles due to the decreasing particle size as a result of annealing and the scattering

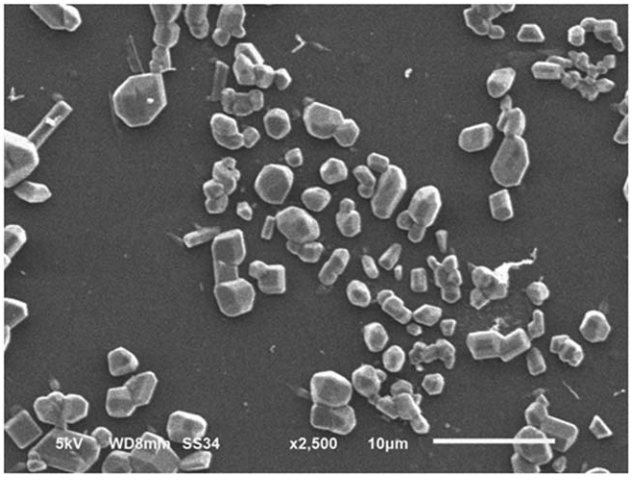


FIG. 6. SEM image of the composite film with 10 PS(wt%) content annealed in IRH system at 60°C.

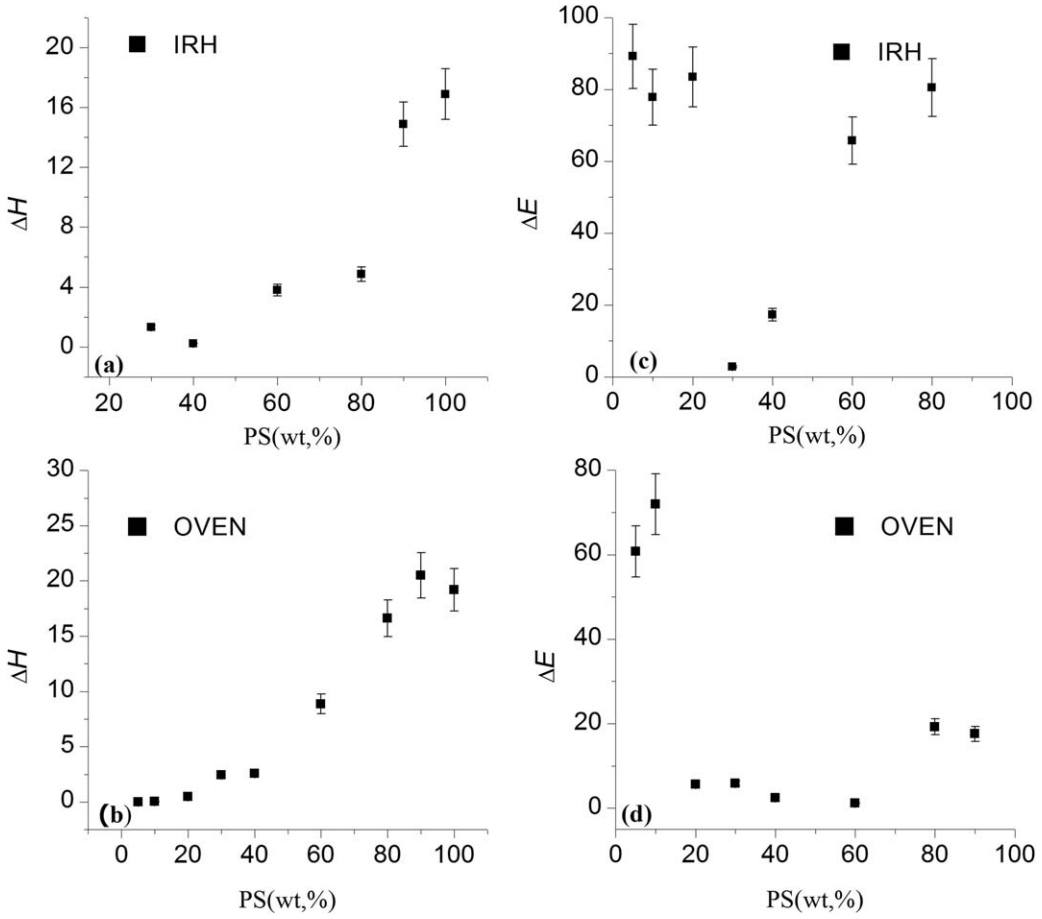


FIG. 7. Void closure (ΔH), and interdiffusion (ΔE) activation energies versus PS (wt%) content for the films annealed in IRH system (a and c) and in the oven (b and d).

behavior of the PS particles at low concentrations. This situation is clearly visible in Fig. 6. Here, the average particle size of the PAAm particles were decreased as a result of annealing at 60°C when compared with the images give in Fig. 1a. After 60% PS content, the PS particles become dominant in the system and turn the structure more homogeneous nature that leads the transmitted light intensity increase again upon annealing at the temperatures above 100°C. Above 200°C, I_{tr} increases with increasing PS content as expected, because the temperatures are high enough to make the films homogeneous for each PS content. Here, another point, which supports that the film formation process is performed at lower temperatures in IRH sytem, is the plots given in Fig. 5c and f. As seen from these plots, the film structure reached at 270°C in the oven has already been reached at 210°C in the IRH heating system.

Calculation of the Activation Energies

The activation energies for the void closure and the interdiffusion processes are calculated by using the following equations [30, 32]:

$$I_{tr}(T)=S(t)\exp\left(-\frac{3\Delta H}{kT}\right) \quad (1)$$

$$I_{tr}(T)/I_{tr}(\infty)=A\exp\left(-\frac{\Delta E}{2k_BT}\right) \quad (2)$$

where $S(t)=(yt/2AC)^3$, k is the Boltzmann's constant, ΔH is the void closure energy, and I_{tr} is the transmittance at 800 nm. By using the least square fitting, the calculated activation energies for the PS and PS/PAAm films annealed by the convective heating in the oven and IRH were given in Fig. 7.

Here it has to be noted that the activation energies for the void closure, were found to be different for two different annealing techniques in Fig. 7 The activation energies for the void closure calculated for IRH are smaller than those calculated for the standart heating in the oven (Fig. 7a and b) and Table 1, 2). This result directly indicates that the void closure process can be performed faster by IRH technique for all composite films. This may be due to the difference between the transmission mechanisms of the energy to the film. In the standard heating technique in the oven, the thermal energy is transmitted to the film as convection, i.e., through the molecules inside the oven and the molecules of the substrate. However, in the IRH system, the thermal energy is transmitted to the film as electromagnetic in nature. In this case, electromagnetic wave directly interacts with the molecules of the polymers in the film and excites the vibrational modes of the molecules which results in increasing kinetic energy and thus increasing temperature.

 DOI 10.1002/pen

TABLE 1. Experimentally calculated void closure (ΔH) and interdiffusion (ΔE) activation energies of the films annealed in IRH system.

PS (% wt)	ΔH_1(kcal/mol)	ΔH_2(kcal/mol)	ΔE_1(kcal/mol)	ΔE_2(kcal/mol)
5	X	X	89.21 ± 6.60	2.36 ± 0.13
10	X	X	77.77 ± 2.70	6.49 ± 0.24
20	X	X	83.44 ± 10.00	4.3 ± 0.10
30	1.31 ± 0.49	X	2.73 ± 0.10	X
40	0.23 ± 0.06	X	1.29 ± 0.10	X
60	3.79 ± 0.35	X	65.78 ± 2.20	X
80	4.84 ± 0.06	X	80.47 ± 5.10	X
90	14.88 ± 0.08	0.14 ± 0.03	X	X
100	16.88 ± 2.60	0.67 ± 0.06	X	X

The time required for this interaction is shorter than the time required for the interaction in the oven. It is also seen that ΔH values are increasing with the increasing PS content for both annealing techniques. This result is understandable because agglomeration in the composite matrix which is dominant up to T_h is making harder to bring the spherical particles together. In other words, inclusion of PS delays the void closure processes and more energy is required to overcome this energy barrier.

However, ΔE values are getting smaller with the increasing PS content up to 30 PS (wt%) for IRH and 60 PS (wt%) for the oven (Fig. 7c and d). After decreasing of ΔE below these certain PS contents, it starts to increase again. This shows that the contribution of PS particles until a critical concentration makes the chain transfer between the particles easier at high temperatures for both heating sytems. This result is consistent with Fig. 2 where I_{tr} for the films annealed in IRH drops to the minimum value at lower temperatures than those of the films annealed in the oven. This decrease in I_{tr} is probably because of the physical deformation of the film because some dark spots were observed on the surface of the PS/PAAm film annealed by IRH after a certain temperature. Before the maximum I_{tr}, probably the interdifussion processes occur very fast and nearly simultaneously. Therefore, it cannot be possible to distinguish these processes during the film formation for the PS/PAAm composite films annealed by IRH. It has to be noticed that this result is valid for the high temperatures. However, the standart heating in the oven starts to become effective for the higher PS content, again. It means that IRH system is having difficulty to supply the required energy for the polymer chain transportation between the particles of the composite latex for high PS content.

In addition, ΔE values are comparably bigger than ΔH values for the two different heating systems. It is quite reasonable to accept that small chain segment (minor chain) needs much less energy to execute its motion than the energy needed to cross the center of mass of a chain through the particle-particle interfaces.

Another interesting result from the Table 1 that while the film formation processes is completed in one stage in both void cloure and interdiffusion processes in the oven, this process is completed in two stages for both void closure and interdiffusion processes by IRH.

TABLE 2. Experimentally calculated void closure (ΔH) and interdiffusion (ΔE) activation energies of the films annealed in the oven.

PS % wt	ΔH(kcal/mol)	ΔE(kcal/mol)
5	$(9.93 \pm 1.00) \times 10^{-3}$	60.77 ± 3.40
10	$(2.00 \pm 0.20) \times 10^{-2}$	71.93 ± 3.37
20	0.49 ± 0.03	5.64 ± 0.19
30	2.44 ± 0.18	5.87 ± 0.32
40	2.58 ± 0.21	2.46 ± 0.49
60	8.87 ± 1.22	1.23 ± 0.24
80	16.62 ± 2.23	19.26 ± 1.10
90	25.91 ± 5.80	17.57 ± 1.32
100	19.19 ± 2.23	X

CONCLUSIONS

In the present work, the film formation process of the PS/PAAm composite matrix and the effect of the different annealing systems, convective heating in oven and in IRH system with IR lamp, on the latex film formation were studied. The results of the experiments performed in this study lead to the following conclusions.

i. The transport of the thermal energy is more efficient in the IRH system. This is due to the absorption of the electromagnetic wave by the molecules in the films.
ii. The time required for the film formation in IRH system is shorter than the time required for the film formation in the traditional oven. This is directly related to the result given in (i). Since the energy transport is more efficient and it is directly transmitted to the molecules of the films as electromagnetic in IRH, the time required for the film formation decreases in IRH system. In the standard heating in the oven, the thermal energy is transferred through the molecules of air inside the oven and through the molecules of the substrate. This mechanism makes the required time for the film formation longer when compared with the IRH system.
iii. The result given in (i) also causes a decrease in the required energy and the temperature for the film formation in IRH system. This point was clearly observed by the SEM images and from the transmittance measurements.

ACKNOWLEDGMENTS

We want to thank Yildiz Tecnical University, Coordination of Scientific Research Projects for financial supporting of our project numbered 2016-01-01-KAP03.

REFERENCES

1. D. Chandra, S. Yang, and P. Lin, *Appl. Phys. Lett.*, **91**, 251912 (2007).
2. H.E. Jeong, M.K. Kwak, and K.Y. Suh, *Langmuir*, **26**, 2223 (2010).

3. E. Menard, M.A. Meitl, Y. Sun, J.-U. Park, D.J.-L. Shir, Y.-K. Nam, S. Jeon, and J.A. Rogers, *Chem. Rev*., **107**, 1117 (2007).
4. http://sffsymposium.engr.utexas.edu/Manuscripts/2006/2006-68-Wimpenny.pdf. DeMontfort University Leicester, UK (Accessed September, 2006).
5. www.noblelight.net (Accessed February, 2014).
6. E. Gonzalez, M. Paulis, M.J. Barandiaran, and J.L. Keddie, *Langmuir*, **29**, 2044 (2013).
7. B. Galindo, A. Benedito, F. Ramos, and E. Gimenez, *Polym. Eng. Sci*., **56**, 1321 (2016).
8. M. Fyrillas, G. Georgiou, D. Vlassopoulos, and S. Hatzikiriakos, *Polym. Eng. Sci*., **39**, (1999).
9. P.R. Sperry, B.S. Snyder, M.L. O'Dowd, and P.M. Lesko, *Langmuir*, **10**, 2619 (1994).
10. J.K. Mackenzie, and R. Shuttleworth, *Phys. Soc*., **62**, 838 (1949).
11. J.N. Yoo, L.H. Sperling, C.J. Glinka, and A. Klein, *Macromolecules*, **24**, 2868 (1991).
12. O. Pekcan, *Trends Polym. Sci*., **2**, 236 (1994).
13. S.T. Eckersley, and A. Rudin, *Prog. Org. Coat*., **23**, 387 (1994).
14. L.A. Cannon, and R.A. Pethrick, *Macromolecules*, **32**, 7617 (1999).
15. Y. Chevalier, *Trends Polym. Sci*., **4**, 197 (1996).
16. O. Pekcan, M.A. Winnik, and M.D. Croucher, *Macromolecules*, **23**, 2673 (1990).
17. S. Ugur, O. Yargı, E. Gunister, and O. Pekcan, *Appl. Clay Sci*., **42**, 39 (2008).
18. J.L. Keddie, P. Meredith, R.A.L. Jones, and A.M. Donald, *Macromolecules*, **28**, 2673 (1995).
19. E. Arda, V. Bulmus, E. Piskin, and O. Pekcan, *J. Colloid Interface Sci*., **213**, 160 (1999).
20. E. Arda, and O. Pekcan, *Polymer*, **42**, 7419 (2001).
21. E. Arda, F. Ozer, E. Piskin, and O. Pekcan, *J. Colloid Interface Sci*., **233**, 271 (2001).
22. O. Pekcan, and E. Arda, *J. Appl. Polym. Sci*., **70**, 339 (1998).
23. P.A. Steward, J. Hearn, and M.C. Wilkinson, *Polym. Int*., **38**, 23 (1995).
24. Y. Chevalier, C. Pichot, C. Graillat, M. Joanicot, K. Wong, J. Maquet, P. Lindner, and B. Cabane, *Colloid Polym. Sci*., **270**, 806 (1992).
25. Y. Yang, and M.C. Gupta, *Nano Lett*., **5**, 2131 (2005).
26. A. Afzal, A. Kausar, and M. Siddiq, *Polym-Plast Technol Eng*, **55**, 1988 (2016).
27. V.K. Thakur, M.K. Thakur, P. Raghavan, and M.R. Kessler, *ACS Sustain. Chem. Eng*., **2**, 1072 (2014).
28. F. Ruffino, V. Torrisi, G. Marletta, and M.G. Grimaldi, *Appl. Phys. A*, **107**, 669 (2012).
29. A. Panwar, V. Choudhary, and D.K. Sharma, *J.Reinf. Plast. Comp*, **30**, 446 (2011).
30. O. Yargi, S. Ugur, and O. Pekcan, *Polym. Compos*, **35**, 817 (2014).
31. O. Yargi, A. Gelir, M. Ozdogan, C. Nuhoglu, and A. Elaissari, *J. Appl. Polym. Sci*, **133**, 15 (2016).
32. E. Arda, S. Kara, and O. Pekcan, *J. Polym. Sci. Part B: Polym. Phys*., **45**, 2918 (2007).

 DOI 10.1002/pen